

Pictures of hyperbolic dynamical systems

Yves Coudene

*IRMAR, Université Rennes 1, campus beaulieu, bat.23
35042 Rennes cedex, France
yves.coudene@univ-rennes1.fr*

Abstract

We create computer-generated pictures of the following uniformly hyperbolic systems : the attractor derived from Anosov, the Plykin attractor and a Smale horseshoe. These systems provide simple examples on which to test computer programs devoted to simulation of “chaotic” dynamical systems.

1 Introduction

Computer-generated pictures of fractals and attractors are quite common on the internet. The *mandelbrot set* [Ma83], the *Lorentz attractor* [Lo63], the *Feigenbaum bifurcation* [Fei78] and the *Henon attractor* [He76] are amongst the most represented dynamical systems on the web. Pictures and computer experiments have proven to be quite useful for their study. In some cases, computer-assisted proofs of their “chaotic” behaviour are the only proofs available.

These systems all fall in the category of systems exhibiting non-uniformly hyperbolic behaviour. Their study is modelled on the theory of uniformly hyperbolic dynamical systems, and try to recover some of the most prominent features of the hyperbolic theory : invariant SRB measures, bernoullicity of these measures, distribution results concerning the repartition of typical orbits, etc.

The modern theory of uniformly hyperbolic systems goes back to the middle of the twentieth century, with the work of D.V. Anosov [An67], S. Smale [Sm67]. It is now a well established theory, and gives a pretty complete description of the dynamics of smooth systems, whose differential is uniformly contracting and dilating on two invariant complementary sub-bundles of the tangent space. The theory provides numerous examples of non-trivial attractors, and gives a nice description of the dynamic on these attractors, by the use of a symbolic model.

As strange as it may seem, there are almost no pictures of these uniformly hyperbolic attractors. There may be several reasons for that ; the theory was build during the sixties, seventies ; at that time, computers were not powerful enough to handle the computations. Also computer experiments are usually focused on systems of physical origin. These systems are often of the non-uniformly hyperbolic type. One of the goal of this article is to provide computer-generated pictures of uniformly hyperbolic dynamical systems. Another goal is to show that we are far from understanding everything about them. We think that these pictures may help in pointing out where are the remaining difficulties, and how to solve them.

Three systems are described in this article : the *attractor derived from Anosov*, the *Plykin attractor*, and a *Smale horseshoe*. From the numerical viewpoint, we think they have a great virtue : their statistical properties have been extensively studied and all possess complete rigorous mathematical proofs. Hence they provide

simple examples on which testing the many computer programs devised for the study of more complicated dynamical systems.

2 Attractors derived from Anosov

The first example is due to S. Smale [Sm67] ; it is obtained by perturbing an Anosov diffeomorphism. Hence it is called an *attractor derived from Anosov*. This attractor is defined on the two-dimensional torus \mathbf{T}^2 . The torus may be seen as a product of two circles $\mathbf{S}^1 \times \mathbf{S}^1$, or as the quotient of the plane \mathbf{R}^2 by the subgroup \mathbf{Z}^2 of points with integer coordinates : $\mathbf{T}^2 \simeq \mathbf{R}^2/\mathbf{Z}^2$.

2.1 Hyperbolic automorphism of the torus

We first need some properties of the matrix $A = \begin{pmatrix} 2 & 1 \\ 1 & 1 \end{pmatrix}$. Let us denote the golden mean by $\lambda = \frac{1+\sqrt{5}}{2} \simeq 1.618$. The matrix A admits two eigenvalues λ^2 and λ^{-2} ; the associated eigenvectors are $\mathbf{e}_u = \frac{1}{\sqrt{1+\lambda^2}} \begin{pmatrix} \lambda \\ 1 \end{pmatrix}$ and $\mathbf{e}_s = \frac{1}{\sqrt{1+\lambda^2}} \begin{pmatrix} -1 \\ \lambda \end{pmatrix}$, and the following relation holds :

$$\begin{pmatrix} 2 & 1 \\ 1 & 1 \end{pmatrix} = \frac{1}{\sqrt{1+\lambda^2}} \begin{pmatrix} \lambda & -1 \\ 1 & \lambda \end{pmatrix} \begin{pmatrix} \lambda^2 & 0 \\ 0 & \lambda^{-2} \end{pmatrix} \frac{1}{\sqrt{1+\lambda^2}} \begin{pmatrix} \lambda & 1 \\ -1 & \lambda \end{pmatrix}$$

The action of the matrix $\begin{pmatrix} 2 & 1 \\ 1 & 1 \end{pmatrix}$ on the plane gives an invertible transformation on the torus \mathbf{T}^2 , called a *hyperbolic toral automorphism*. This transformation is an Anosov diffeomorphism : there are two invariant uniformly contracting and dilating sub-bundles in the tangent space. The contracting one is directed by \mathbf{e}_u at each point, the dilating one by \mathbf{e}_s .

The following can be shown about the dynamics of the toral automorphism :

- the periodic points are dense ;
- there exists a point whose orbit is dense ;
- there are many ergodic invariant probability measures with full support ;

These properties are shared by all transitive Anosov diffeomorphisms, and can be obtained by the use of a symbolic model. For the hyperbolic toral automorphisms, this model was first constructed by R. Adler and B. Weiss [AW67]. It was later extended by Sinai to all transitive Anosov diffeomorphisms [Si68]. The book of R. Bowen [Bo75] contains a presentation of these results, as does the survey of J.C. Yoccoz [Yoc95].

We describe briefly how to build this symbolic model for the automorphism $\begin{pmatrix} 2 & 1 \\ 1 & 1 \end{pmatrix}$. Let us begin with the simpler example of the multiplication by 2 defined on \mathbf{R}/\mathbf{Z} . The base two expansion of real numbers gives a surjective map from the set of sequences of zeros and ones to the space \mathbf{R}/\mathbf{Z} .

$$(a_n)_{n \in \mathbf{N}^*} \mapsto \sum \frac{a_n}{2^n}$$

Multiplication by two mod one on the reals amounts to shifting the digits of the expansion to the left. Hence we obtain a conjugation between the multiplication by two on \mathbf{R}/\mathbf{Z} and the shift on the space of sequences of zeroes and ones.

The properties described earlier are easy to prove now : two points are 2^n -close together if their n first digits coincide. Given any sequence of zeros and ones, we may take the first n terms of the sequence and repeat them periodically. This gives a new sequence, which is periodic and close to the previous one. Also a dense sequence is obtained by concatenating all words built of zeroes and ones : 0 1 00 01

10 11 etc. Finally, for any $p \in]0, 1[$, there is a probability measure giving probability p to 0 and $1 - p$ to 1. The law of large number asserts that this measure is ergodic.

In the base $(\mathbf{e}_u, \mathbf{e}_s)$, the action of the matrix $\begin{pmatrix} 2 & 1 \\ 1 & 1 \end{pmatrix}$ is multiplication by λ^2 on the first coordinate, and multiplication by λ^{-2} on the other coordinate. Now any real number $x > 0$ admits a decomposition in base λ : $x = \sum a_n \lambda^{-n}$ for some sequence $a_n \in \{0, 1\}$ (just define a_n recursively by $a_{n+1} = E((x - \sum^n a_k \lambda^k)/\lambda^{n+1})$ where E is the integer part, and note that not all sequences occur : if $a_n = 1$, $a_{n+1} = 0$). So, given two sequences of zeroes and ones, we may associate a point on the torus whose first coordinate in the base $(\mathbf{e}_u, \mathbf{e}_s)$ admits the first sequence as its decomposition in base λ , and whose second coordinate is given by the second sequence. Applying the matrix amounts to shifting the sequences twice to the right and to the left respectively. One checks that the two digits lost on the left-shifted sequence are recovered on the other sequence. This gives the desired symbolic model and implies the properties discussed above.

2.2 The perturbation

We now add a term to the diffeomorphism, so as to transform the fixed point $\begin{pmatrix} 0 \\ 0 \end{pmatrix}$ into an attracting fixed point.

$$f_1 : \begin{pmatrix} x \\ y \end{pmatrix} \mapsto \begin{pmatrix} 2 & 1 \\ 1 & 1 \end{pmatrix} \begin{pmatrix} x \\ y \end{pmatrix} + \frac{p_1}{1 + \lambda^2} k(x/a)k(y/a) \begin{pmatrix} \lambda^2 & \lambda \\ \lambda & 1 \end{pmatrix} \begin{pmatrix} x \\ y \end{pmatrix}$$

with $k(x) = (1 - x^2)^2 \mathbf{1}_{[-1,1]}(x)$ used as a C^1 “bump” function. The parameter a controls the extent of the perturbation, the parameter p_1 controls its amplitude. The additional term only modifies the dominant eigenvalue. The differential at the fixed point $\begin{pmatrix} 0 \\ 0 \end{pmatrix}$ is now conjugated to $\begin{pmatrix} \lambda^2 + p_1 & 0 \\ 0 & \lambda^{-2} \end{pmatrix}$.

Note that $\lambda_2 \simeq 2.618$; so if we choose $p_1 = -2.2$, the point $\begin{pmatrix} 0 \\ 0 \end{pmatrix}$ becomes an attracting fixed point. If the parameter a is less than 0.5, say $a = 0.4$, the periodic point $\begin{pmatrix} 0.5 \\ 0.5 \end{pmatrix}$ of A is again a hyperbolic periodic point for f_1 . Hence not all points are attracted by $\begin{pmatrix} 0 \\ 0 \end{pmatrix}$. So, we may expect to see an open set of points attracted to the point $\begin{pmatrix} 0 \\ 0 \end{pmatrix}$, whereas there is still an invariant compact set on which the dynamics retains some of the features of the hyperbolic toral automorphism. This is indeed what happens for the chosen set of parameters. The basin of attraction of the point $\begin{pmatrix} 0 \\ 0 \end{pmatrix}$ is depicted in figure 1.

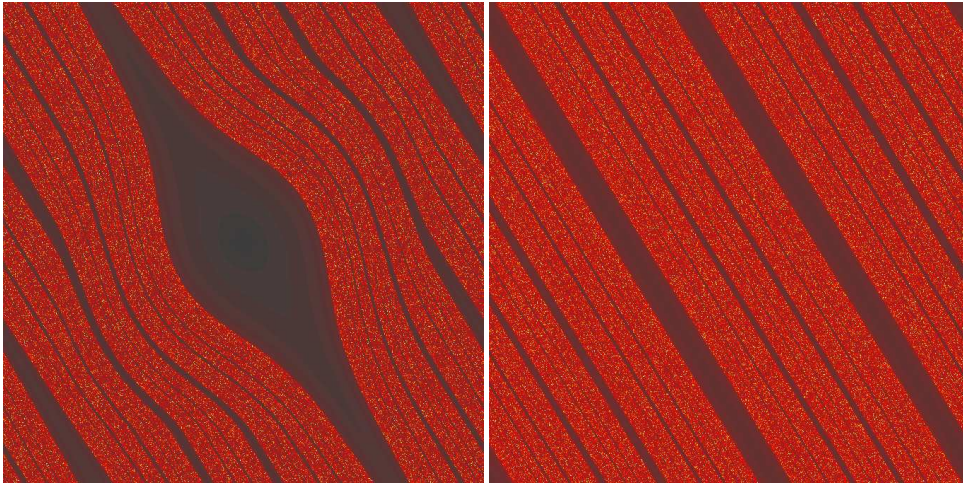


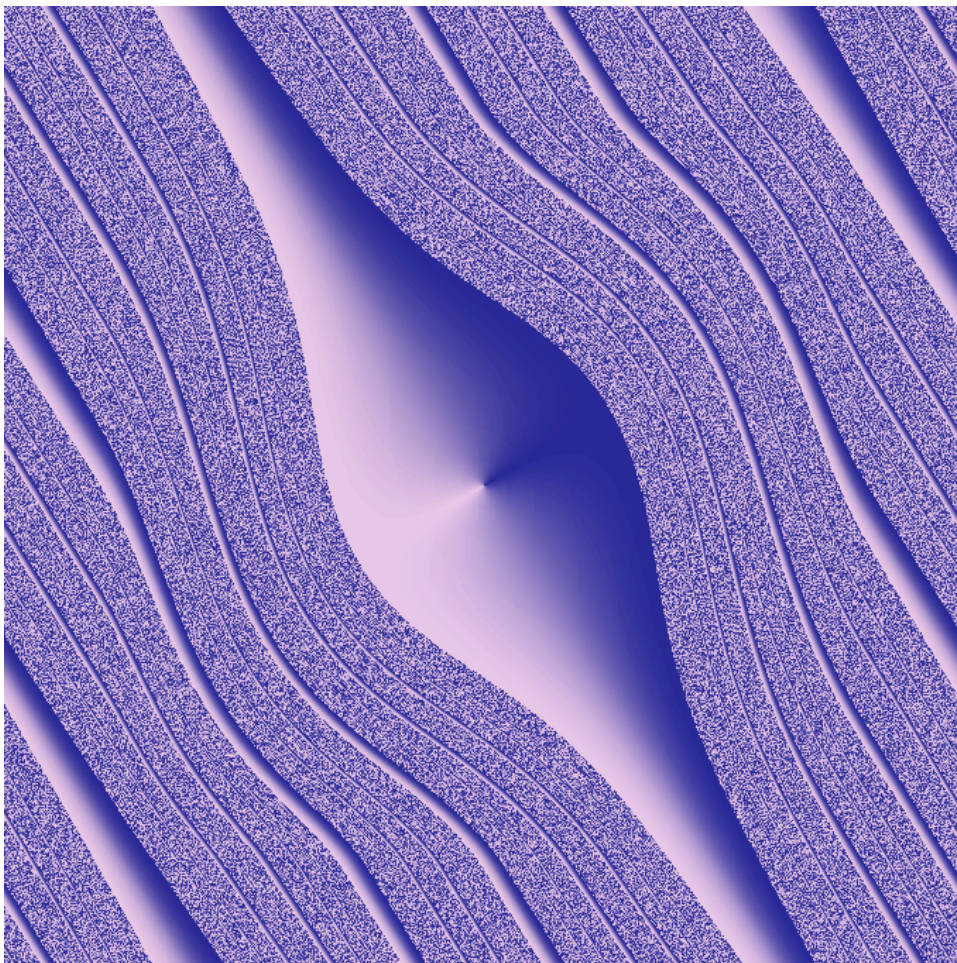
Figure 1 \triangle

\triangle Figure 2

Figure 2 is an enlargement of a small part of figure 1 , centered on the point $(\frac{0.5}{0.5})$. It reveals a structure of the type “Cantor times interval” in the complementary of the basin of attraction.

Let us explain how it was obtained. For each pixel on the picture, we calculate the number of iterations needed to reach a small neighborhood of the attracting fixed point $(\frac{0}{0})$, say the disk $\{(x, y) \mid x^2 + y^2 < 0.0001\}$. The pixel is colored according to that number of iterations : points that take less than ten iterations to reach the small disk are colored in black. The intensity of the color then increases until thirty iterations are needed, in which case the pixel appears in red. Pixels in yellow need around seventies iterations. Points needing more than two hundreds iterations should appear in bright white, although they are hard to spot on the picture. Of course, points needing more than ten iterations to reach the small disk around the attracting fixed point are very close to the boundary of the basin of attraction ; thus the colored area on figure 1 almost coincides with the complementary of the basin.

Other algorithms can be used to get a glimpse at that basin of attraction. In figure 3, we first color the small disk $\{(x, y) \mid x^2 + y^2 < 0.0001\}$ radially. Points in the direction of $-\mathbf{e}_u$ are colored in white ; the color smoothly fades until it reaches dark blue, which is attained for points in the direction of \mathbf{e}_u . Each pixel is then colored according to the color of the first iterate which falls in the small disk.



△ Figure 3

2.3 Properties of the attractor

We now consider the inverse of the transformation f_1 , instead of f_1 . The point $\begin{pmatrix} 0 \\ 0 \end{pmatrix}$ is a repelling fixed point for f_1^{-1} . The complementary of its basin of repulsion is an attractor ; it is an *attractor derived from Anosov*.

Let us denote $D = \{(x, y) \mid x^2 + y^2 < 0.0001\}$. The *basin of attraction* B of f_1 is the set of all points admitting an iterate which falls in D . Hence we have $B = \bigcup f_1^{-n}(D)$. the basin B is a countable increasing union of open sets diffeomorphic to a disk ; hence it is an immersed disk. On the set B , the transformation f_1 is topologically conjugated to its linearization $D_{(0,0)}f_1$. In other words, there is an homeomorphism $h : B \rightarrow \mathbf{R}^2$ such that $h \circ f_1 \circ h^{-1} = \begin{pmatrix} \lambda^2 + p_1 & 0 \\ 0 & \lambda^{-2} \end{pmatrix}$; recall that $\lambda^2 \simeq 2.618$, $p_1 = -2.2$ and $\lambda^{-2} \simeq 0.382$.

The existence of such a conjugacy in a small neighborhood of the attracting fixed point follows from the Hartman-Grossman theorem. It is then extended to the whole basin of attraction by defining $h = f_1^{-n} \circ h \circ f_1^n$ on the iterates of that conjugacy neighborhood. As a consequence, we see that the open set $U = \mathbf{T}^2 - \begin{pmatrix} 0 \\ 0 \end{pmatrix}$ satisfies the property :

$$B^c = \bigcap_{n \in \mathbf{N}} f_1^n(U).$$

This means that the invariant compact set B^c is an attractor for f_1^{-1} , whose basin of attraction coincides with $\mathbf{T}^2 - \begin{pmatrix} 0 \\ 0 \end{pmatrix}$.

The restriction of the tangent space to the set B^c can be decomposed into two invariant one-dimensional subbundles, that are respectively uniformly contracted and dilated by the differential of the transformation f_1 . The proof can be found in [PaDM82]. In fact, the bundle directed by \mathbf{e}_u is again invariant by Df_1 , and gives the contracting bundle of f_1^{-1} . The dilating bundle is obtained by an invariant Cone field criterion.

The set B is an attracting compact invariant hyperbolic set for f_1^{-1} . The general theory of uniformly hyperbolic systems then provides a symbolic model for the dynamics of f_1^{-1} in restriction to B^c . This model allows to recover stochastic properties similar to the one satisfied by the hyperbolic automorphism of the torus.

3 The Plykin attractor

The attractor derived from Anosov lives on the torus. One can ask if there are uniformly hyperbolic attractors on the sphere. The first example of such a system was given by Plykin [Ply74] ; it can be obtained from the attractor derived from Anosov by realizing the sphere as a quotient of the torus.

3.1 Second deformation

We first make another deformation to the map f_1 , in order to obtain other attracting basins. The orbit of the point $\begin{pmatrix} 0.5 \\ 0.5 \end{pmatrix}$ is periodic of period three under the transformation f . Indeed we have :

$$f_1 \begin{pmatrix} 0.5 \\ 0.5 \end{pmatrix} = \begin{pmatrix} 0.5 \\ 0 \end{pmatrix}, \quad f_1 \begin{pmatrix} 0.5 \\ 0 \end{pmatrix} = \begin{pmatrix} 0 \\ 0.5 \end{pmatrix}, \quad f_1 \begin{pmatrix} 0 \\ 0.5 \end{pmatrix} = \begin{pmatrix} 0.5 \\ 0.5 \end{pmatrix}.$$

Let us denote the integer part of some real number x by $E(x)$. The following change of variables :

$$\begin{cases} x_2 = x - 0.5 E(2x + 0.5) \\ y_2 = y - 0.5 E(2y + 0.5) \end{cases}$$

sends the three periodic points to the center $\begin{pmatrix} 0 \\ 0 \end{pmatrix}$. In order to transform these points into attracting periodic points, we add another term to the map f_1 , and consider the map $f_2 : \mathbf{T}^2 \rightarrow \mathbf{T}^2$ sending $\begin{pmatrix} x \\ y \end{pmatrix}$ to :

$$\begin{pmatrix} 2 & 1 \\ 1 & 1 \end{pmatrix} \begin{pmatrix} x \\ y \end{pmatrix} + \frac{p_1 k(\frac{x}{a}) k(\frac{y}{a})}{1 + \lambda^2} \begin{pmatrix} \lambda^2 & \lambda \\ \lambda & 1 \end{pmatrix} \begin{pmatrix} x \\ y \end{pmatrix} + \frac{p_2 k(\frac{x_2}{b}) k(\frac{y_2}{b})}{1 + \lambda^2} \begin{pmatrix} \lambda^2 & \lambda \\ \lambda & 1 \end{pmatrix} \begin{pmatrix} x_2 \\ y_2 \end{pmatrix}$$

We take $a = 0.4$ and $b = 0.1$, so that the two perturbations do not interfere. The differential of f_2 at the three periodic points is conjuguated to $\begin{pmatrix} \lambda^2 + p_2 & 0 \\ 0 & \lambda^{-2} \end{pmatrix}$. The periodic orbit of period three becomes attractive if, for example, $p_2 = -2.2$.

The result is depicted in Figure 4. That figure is centered on the periodic point $\begin{pmatrix} 0.5 \\ 0.5 \end{pmatrix}$. Its basin of attraction appears in black. The algorithm used for that picture is similar to the algorithm of Figure 1. The inverse of the third iterate of f_2 , f_2^{-3} , admits four repelling fixed points ; the complementary of the basin of repulsion of these four points is an attractor, on which the dynamics enjoys properties similar to the hyperbolic automorphism of the torus. The four basins of repulsion are depicted in different colors on figure 5.

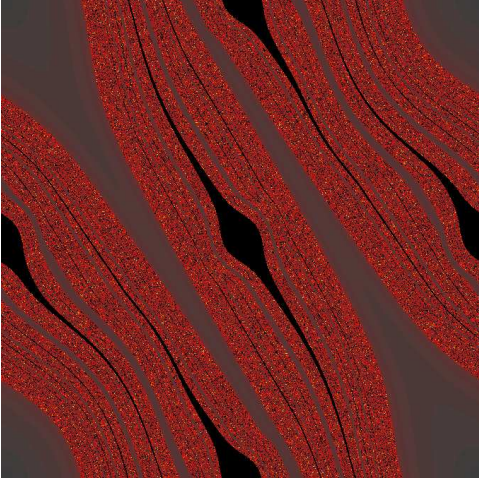
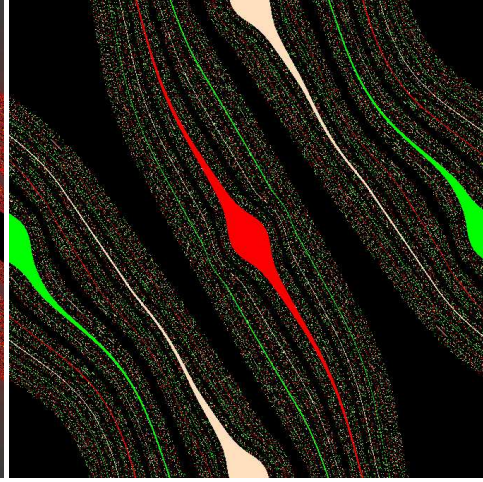


Figure 4 \triangle



\triangle Figure 5

3.2 From the torus to the sphere

We now consider the symmetry on the torus given by $(x, y) \mapsto (-x, -y)$. This symmetry has four fixed points, which are precisely the fixed point of f_2 and the three periodic points of period three. We may quotient the torus by this symmetry. The resulting space is topologically a sphere ; from the differential viewpoint, it is a sphere with four conical points. Such a space has an euclidean model, namely the tetrahedron. If we start from the hexagonal torus instead of the usual one , the resulting tetrahedron is regular.

The transformation f_2^{-1} commutes with the symmetry, so it defines a transformation of the tetrahedron, for which the four vertices are repelling fixed points. The *Plykin attractor* is obtained by smoothing the tetrahedron and the transformation f_2^{-1} in a neighborhood of the vertices. Note that if the smoothing is small enough, it takes place in the basins of repulsion of the repelling points, and do not alter the attractor. So, for purpose of representation , this smoothing is irrelevant. Figure 6 gives an explicit model for the tetrahedron, which can be cut and pasted to obtain a representation of the Plykin attractor.

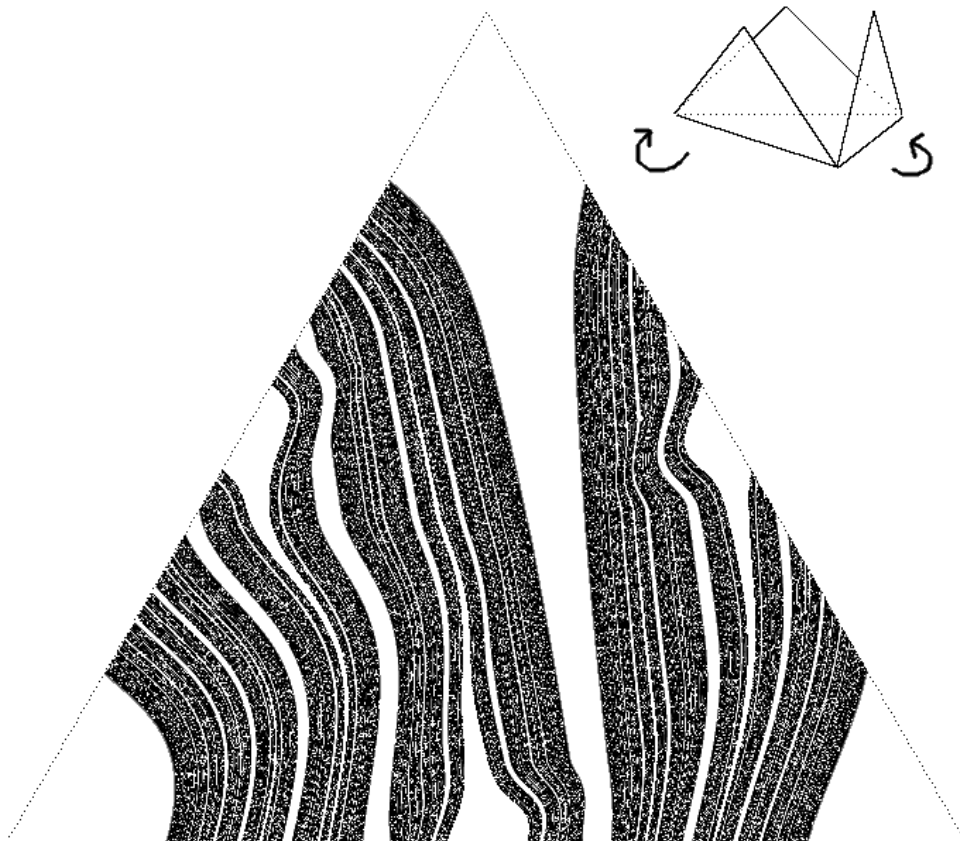


Figure 6 \triangle

3.3 Lakes of Wada

Finally, the sphere or the tetrahedron may be stereographically projected on the plane. The repelling fixed point $(\frac{0}{0})$ on the torus is sent to infinity by the projection. The map obtained from f_2^{-1} is a diffeomorphism of the plane, for which infinity is repelling ; it admits moreover a period three repelling orbit, and the complementary of the basins of repulsion is an attractor which is depicted in Figure 7.

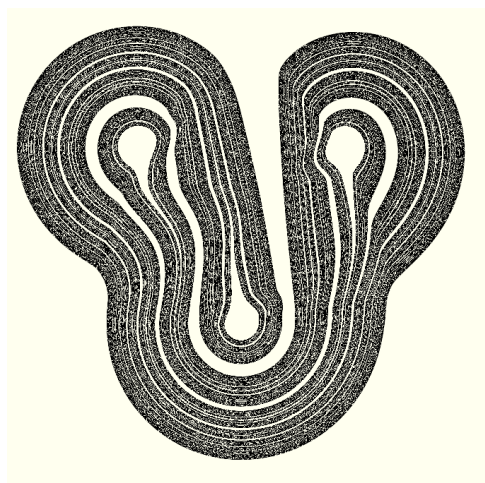
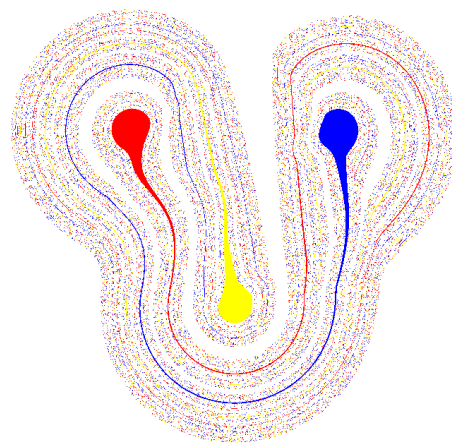


Figure 7 \triangle



\triangle Figure 8

We remark that the basins of repulsion of the transformation form Lakes of Wada : each of the four basins is an immersed disk ; and each of these disks have the same boundary , the attractor itself. In other words, any point on the attractor is accumulated by the four basins of repulsion. Such immersion of disks in the plane was first conceived by L. Brouwer and effectively built by K. Yoneyama [Yon17]. The basins are depicted in different colors on Figure 8.

4 The Smale horseshoe

4.1 Third deformation

We come back to the transformation f_1 on the torus. What happens if the periodic orbit of period three of f_1 is deformed into a repelling periodic orbit instead of an attracting periodic orbit ? Such a deformation can be achieved by adding a third term to the automorphism of the torus :

$$f_3 \begin{pmatrix} x \\ y \end{pmatrix} = f_2 \begin{pmatrix} x \\ y \end{pmatrix} + \frac{p_3 k\left(\frac{x_2}{a}\right)k\left(\frac{y_2}{a}\right)}{1 + \lambda^2} \begin{pmatrix} \cos(p_4) & -\sin(p_4) \\ \sin(p_4) & \cos(p_4) \end{pmatrix} \begin{pmatrix} x_2 \\ y_2 \end{pmatrix}$$

The parameter p_3 determines the amplitude of the perturbation , the parameter p_4 determines its phase. The eigenvalues of Df_3 at the periodic points of period three are equal to $\lambda^2 + p_2 + p_3 e^{ip_4}$ and $\lambda^{-2} + p_3 e^{ip_4}$. We take $p_2 = -2.2$, $p_3 = 0.7$.

Figure 9 shows the result for $p_4 = 0$; the algorithm used is the same as in Figures 1 and 2. The figure is centered on the point $\begin{pmatrix} 0.5 \\ 0.5 \end{pmatrix}$. Note that colors around this point seem to be brighter, compared to Figure 1. Figure 10 shows an enlargement around $\begin{pmatrix} 0.5 \\ 0.5 \end{pmatrix}$, and should be compared with Figure 2. We can see how the basin of attraction of the point $\begin{pmatrix} 0 \\ 0 \end{pmatrix}$ (in black on the picture) is repelled by the point $\begin{pmatrix} 0.5 \\ 0.5 \end{pmatrix}$.

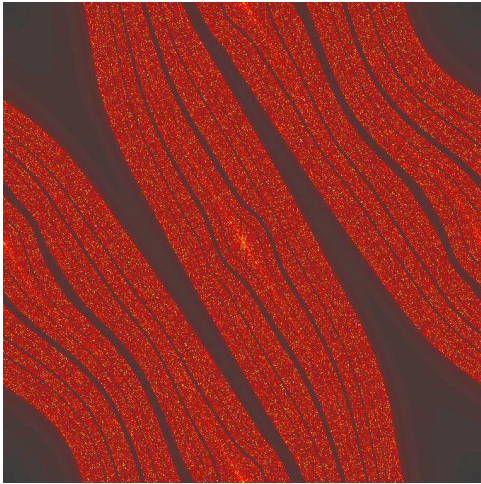
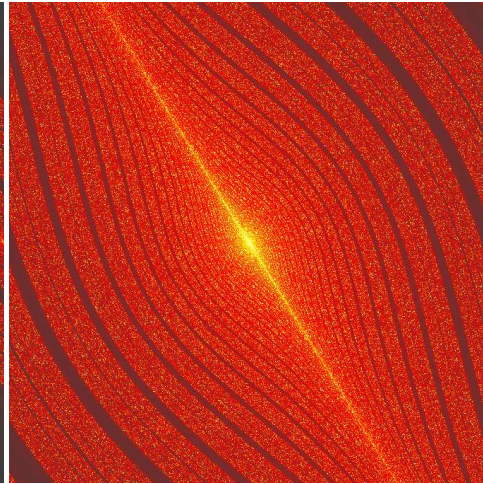


Figure 9 \triangle



\triangle Figure 10

Figures 11 and 12 show the result for $p_4 = 0.6$. Red has been replaced by Blue. The basin of attraction of the point $\begin{pmatrix} 0 \\ 0 \end{pmatrix}$ (dark part of the picture) now turns around the repelling point $\begin{pmatrix} 0.5 \\ 0.5 \end{pmatrix}$.

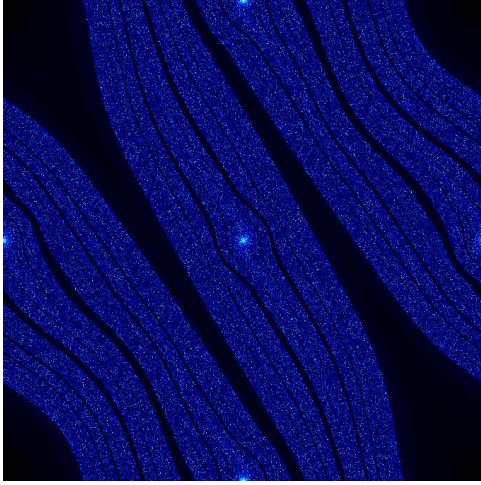
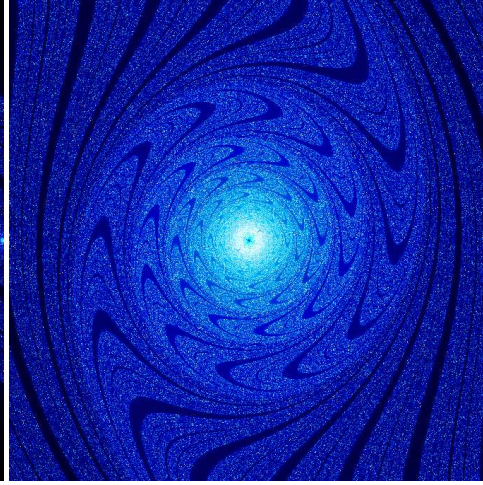


Figure 11 \triangle



\triangle Figure 12

4.2 Horseshoes

The transformation f_3 on the torus induces a mapping on the sphere, which exhibits a “Smale horseshoe”. It possesses a repelling orbit of period three, and the infinity is an attracting fixed point.

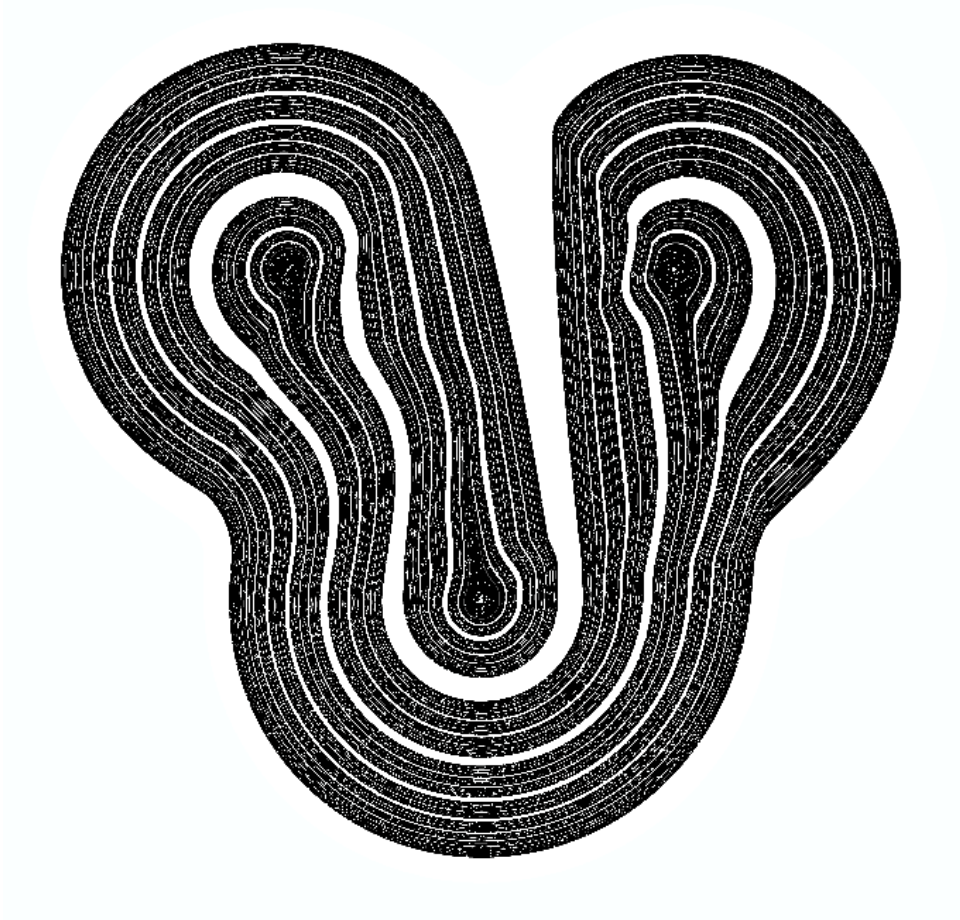


Figure 13 \triangle

The compact set K depicted in Figure 13 ($p_4 = 0$) consists of the points which are not attracted by infinity. This set may be split into three invariant subsets : the repelling orbit of period three ; a Cantor set Ω consisting of the closure of the recurrent points of f_3 (different from the three repelling points) ; and the set of points which are attracted by this Cantor set. The closure of the recurrent points is the set usually called the *horseshoe*. One can show that the transformation g admits an hyperbolic decomposition in restriction to this set. Thus f_3 is an Axiom A diffeomorphism, and the general theory of Axiom A diffeomorphisms provides a symbolic model describing the dynamics of f_3 on Ω .

Figure 14 is a colored version of Figure 13, whereas Figure 15 is an enlargement of Figure 14 around one of the three repelling points. The brighter the points, the longer it takes to reach infinity, hence the closer they are from the set of points not attracted by infinity.

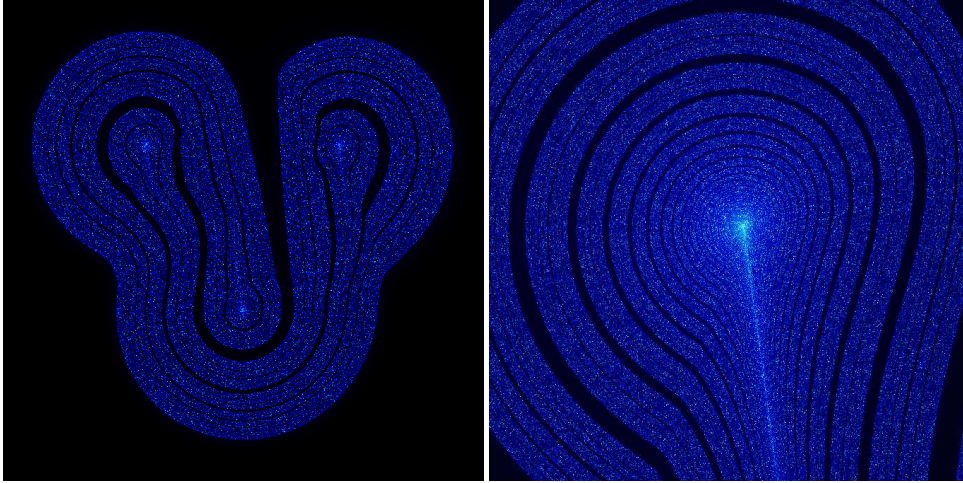


Figure 14 \triangle

\triangle Figure 15

In [Sm67], S. Smale gives a general method for building horseshoes, by “stretching” rectangles. We explain how it relates to the preceding construction.

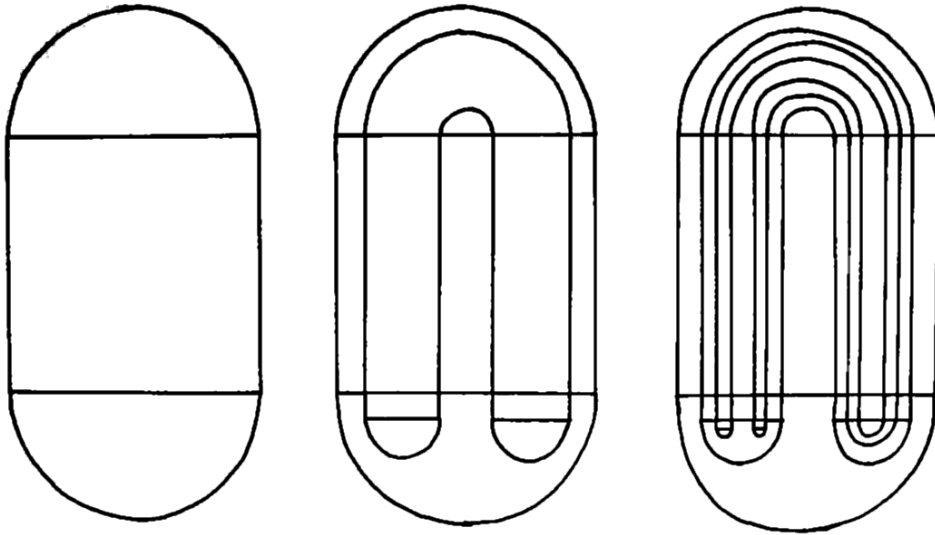


Figure 16 \triangle

Let us describe a continuous transformation from the plane to itself, which gives rise to a Cantor set similar to the one depicted in Figure 13. The set pictured at the left of Figure 16 is denoted by A ; outside this set, the transformation is uniformly contracting. The set itself is uniformly dilated in the vertical direction, and contracted in the horizontal direction. It is then “bent” as depicted in the second picture of Figure 16. The last picture shows what is obtained by iterating another time the transformation. The infinity is an attracting fixed point for the inverse of the transformation, which also possesses a repelling fixed point located in the bottom part of A . The intersection of all the images of A gives a compact set which locally looks like a Cantor set times an interval.

By modifying slightly the preceding construction, we can build a transformation with a period three repelling orbit, and an attracting fixed point at infinity. The picture below shows how the bending is done.

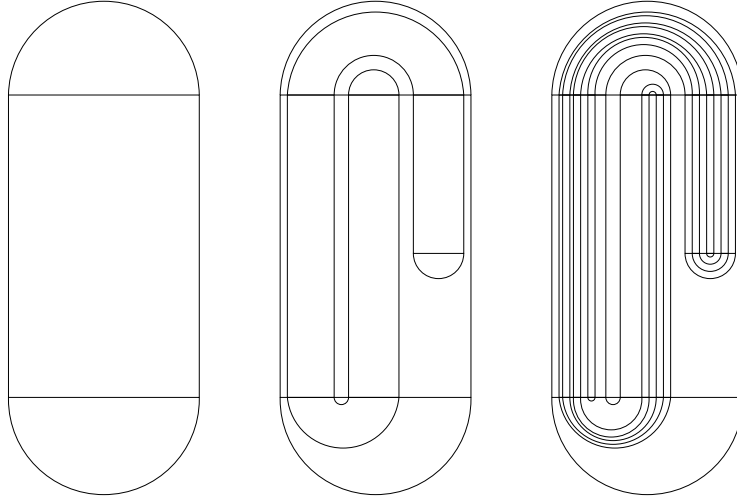
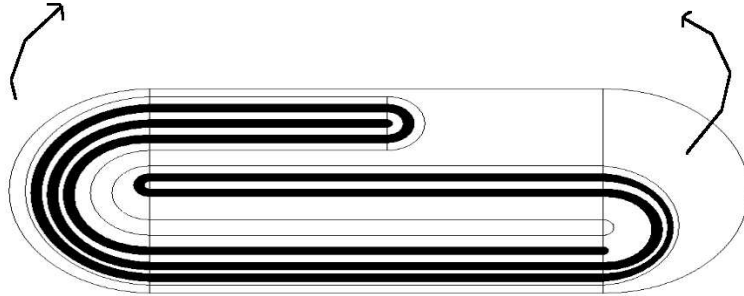


Figure 17 \triangle

Figure 13 is then obtained by bending a last time the resulting compact set, as done on the picture below.



4.3 The dissipative part of the horseshoe

What can be said about the set K (ie the set depicted in Figure 13) ? or from the subset of the torus depicted in Figure 9 or 11, from which K is obtained ? The action of f_3 on this set is totally dissipative, and provides few informations.

On the other hand, there is a flow defined on this compact set. The set K is locally homeomorphic to the product of a Cantor set by an interval, so we may consider translation along this interval. Several parameterizations are possible ; for example, a riemannian metric defined on a neighborhood of K may be used to

obtain a flow ϕ_t parameterized by arc length. The trajectory of some point $x \in K$ under the flow is the projection on the sphere of the stable manifold $W^s(x)$ of the point x , under the action of f_3 :

$$W^s(x) = \{y \in \mathbf{T}^2 \mid d(f_3^n(x), f_3^n(y)) \rightarrow 0 \text{ as } n \rightarrow +\infty\}$$

The flow has three singularities coming from the repelling orbit of f_3 . Note that the points whose stable manifold ends on one of the repelling points $(\frac{5}{5})$, $(\frac{5}{0})$ or $(\frac{0}{5})$, form six immersed one dimensional curves which are dense in K . On the complementary of these points, the flow is continuous.

It is not known whether the flow ϕ_t admits a finite or infinite ergodic invariant measure fully supported on K . Also, studying the statistical distribution of the orbits of the flow is an open problem. Note however that the foliation W^s on $K - \{(\frac{5}{5}), (\frac{5}{0}), (\frac{0}{5})\}$ admits a unique transverse invariant family of measures ; this result is due to R. Bowen and B. Marcus [BM77]. Hence if the measure exists, it is unique.

From the similarities between the pictures obtained for the attractor derived from Anosov and the horseshoe, one may conjecture that there indeed exists a finite measure invariant by the flow, for a suitable parameterization of the flow. Also it should be equidistributed in the sense that, means on increasing pieces of a stable manifold should converge uniformly to the mean with respect to the invariant measure, as soon as the chosen stable manifold is different from the six manifolds ending on a repelling periodic point of period three.

References

- [AW67] R. L. Adler, B. Weiss, Entropy, a complete invariant for automorphisms of the torus, *Proceedings of National Academy of Sciences* **57** (1967), 1573-1576.
- [An67] D.V. Anosov. Geodesic flows on closed riemannian manifolds with negative curvature. *Proc. Steklov Inst. Math* **90**, (1967).
- [Bo75] R. Bowen. Equilibrium states and the ergodic theory of Anosov diffeomorphisms, *Lectures notes in mathematics* **470**, Springer (1975).
- [BM77] R. Bowen, B. Marcus. Unique ergodicity for horocycle foliations, *Israel J. math.* **13**, (1977), 43-67.
- [Fei78] M. J. Feigenbaum. Quantitative universality for a class of nonlinear transformations. *J. Statist. Phys.* 19 (1978), no. 1, 25–52.
- [He76] M. Hénon. A two-dimensional mapping with a strange attractor. *Comm. Math. Phys.* 50 (1976), no. 1, 69–77.
- [Lo63] E. Lorenz. deterministic nonperiodic flow *J. Atmospheric Sci.* **20**, 130-141.
- [Ma83] B. Mandelbrot. On the quadratic mapping $z \rightarrow z^2 - \mu$ for complex μ and z : the fractal structure of its \mathcal{M} set, and scaling. *Order in chaos* (Los Alamos, N.M., 1982). *Phys. D* 7 (1983), no. 1-3, 224–239.
- [Ply74] R. V. Plykin. Sources and sinks of A-diffeomorphisms of surfaces. (Russian) *Mat. Sb. (N.S.)* 94(136) (1974), 243–264, 336.
- [PaDM82] J. Palis, W. de Melo. Geometric theory of dynamical systems. An introduction. Translated from the Portuguese by A. K. Manning. Springer-Verlag, New York-Berlin, 1982.
- [Si68] Y. G. Sinai, Markov partitions and Y-diffeomorphisms. (Russian) *Funkcional. Anal. i Prilozhen* **2** 1968 no. 1, 64–89.

- [Sm67] S. Smale. Differentiable dynamical systems, *Bull. AMS* **73**, (1967), 747-817.
- [Yoc95] J. C. Yoccoz. Introduction to hyperbolic dynamics. Real and complex dynamical systems (Hillerd, 1993), 265–291, NATO Adv. Sci. Inst. Ser. C Math. Phys. Sci., 464, Kluwer Acad. Publ., Dordrecht, 1995.
- [Yon17] K. Yoneyama. Theory of continuous set of points. *Tohoku Math. J.* **11-12**, 43 (1917).